Excitation analysis on resilient mounting eigenmodes of large-bore internal combustion engines

M. Donderer [1,3], **A. Rieß** [1], **U. Waldenmaier** [1], **J. Neher** [2], **S. Ehlers** [3]
[1] MAN Energy Solutions SE, Product Line Four-Stroke - Mechanics & Validation,
Stadtbachstrasse 1, 86153, Augsburg, Germany

[2] Ulm University of Applied Sciences, Department of Structural Mechanics and Acoustics
Prittwitzstrasse 10, 89075, Ulm, Germany

[3] Hamburg University of Technology, Institute for Ship Structural Design and Analysis,
Am Schwarzenberg Campus 4c, 21073, Hamburg, Germany

Abstract
Modern large-bore internal combustion (IC) engines are decoupled from the foundation using resilient rubber mounts. A resiliently mounted engine significantly reduces structure-borne noise (SBN) transmission from the engine as vibration source to the surrounding, e.g. a passenger or cruise ship. During Modal Analysis of such a system, particular Resilient Mounting Eigenmodes due to the rubber elements can be observed which have far lower eigenfrequencies than the engine's structural components. Therefore, it is a common assumption to consider the engine as rigid body in the design of the resilient mounting. This work discusses this simplification by carrying out a Harmonic Response Analysis for a rigid and an elastic engine model. It is shown how elasticity of the engine structure significantly changes the vibration response. Further, it is illustrated that the excitation of Resilient Mounting Eigenmodes is an intrinsic engine property and not coming from e.g. unbalances during the production process or other external sources as commonly assumed.

1 Introduction

The importance of underwater radiated noise (UWN) for commercial shipping has grown to a significant extend over the last years. Nowadays, almost every new built ship is designed with attention to its later UWN characteristics, especially cruise ships [1] and research vessels. On the one hand, this is due to the growing research and knowledge about how noise from shipping negatively affects marine mammals [2, 3, 4, 5], on the other hand it is driven by new legislation and regulations from the International Maritime Organization (IMO) [6] or local authorities, e.g. Vancouver Port [7], which try to overcome the negative effects of UWN on the maritime biosphere. From an engineering point of view, there are several aspects of UWN which can be grouped into the topics

- noise excitation (main engines, auxiliary drives, gensets, propeller, ...)
- noise transmission (structure-borne noise (SBN), air-borne noise (ABN), exhaust gas noise (EGN), design of ship structure, ...)
- noise radiation (design of ship hull)

The overall system regarding the described noise excitation and transmission elements is shown in Figure 1.

In this work, we focus on the topics noise excitation by a resiliently mounted 4-stroke IC main engine and its noise transmission to the ship foundation. The foundation is the point of the ship structure where the main engines are mounted. It is typically stiffer and has a distinct structure compared to the surrounding double-walled ship hull in order to withstand the engine vibrations in an optimized way. The excitation mechanisms

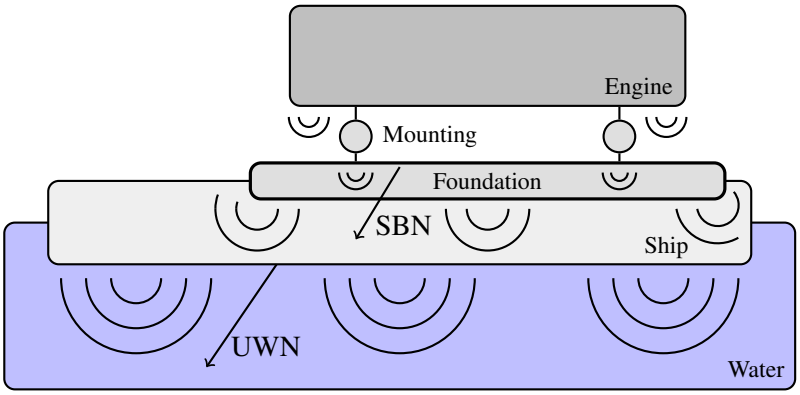

Figure 1: Excitation of UWN by an engine. Vibrations are transmitted through the mounting to the foundation on the ship before they are radiated into water from the ship hull.

(see Section 2) cause the engine structure to vibrate. The vibration shapes are thereby determined by eigenfrequencies and eigenmodes of the engine. In this paper, we use a MAN 12V48/60CR engine as an example. We can group the eigenfrequencies of the engine obtained by Modal Analysis into two parts as in Table 1.

One group are the Elastic Engine Modes defined by the engine structure. The other group are modes determined by the resilient mounting (Resilient Mounting Eigenmodes). The frequencies and mode shapes of this group are determined by the engine mass and the parameters of the resilient mounting, i.e. dynamic rubber stiffness and the number and positioning of the individual rubber elements, and can be treated separately to the remaining Elastic Engine Modes. Moreover, if a proper dimensioned resilient mounting system is used, for many applications the Elastic Engine Modes can be analyzed independently of the remaining system, since a modal decoupling from the ship structure takes place.

Table 1: Eigenfrequencies (EFs) from a MAN 12V48/60CR engine on elastic mounting without further elastic connections to the surrounding, e.g. couplings or compensators.

Type	**Mode #**	**EF** [Hz]
Resilient Mounting Eigenmode	1	2.58
	2	3.13
	3	6.46
	4	6.95
	5	7.46
	6	7.75
Elastic Engine Eigenmode	7	22.05
	8	22.61
	9	23.27
	10	27.57
	⋮	⋮

The treatment of Resilient Mounting Eigenmodes plays a key role in the process of engine-plant integration. Their frequencies lie close to the rotational frequency of the engine and the nearby harmonic orders. Further, since they lie close to the low engine orders, they can have a significant influence on the vibration response or can even dominate it in case of resonance. For those reasons, we will take a closer look at Resilient Mounting Eigenmodes and their excitability during engine operation in the following sections and describe their distinctiveness among all vibration modes of the considered dynamic system. We further describe the effects of treating the engine as a rigid body during the analysis of Resilient Mounting Eigenmodes and show how this assumption can lead to unexpected results. Finally, we illustrate how traditional analytical methods can lead to misleading results in the Response Analysis (RA) of Resilient Mounting Eigenmodes.

2 Methodology

We start with an explanation of the main excitation mechanisms of IC engines. Throughout the paper we refer to an IC engine solely as engine, too.

2.1 Excitation Principles

Through the combustion of liquid or gaseous fuel, an engine delivers mechanical power for propulsion, generation of electric energy or the powering of a variety of machines. During this process, the engine is excited to vibrations by periodic gas forces and oscillating and rotating mass forces. For a single cylinder four-stroke engine, the acting forces are as following.

2.1.1 Single Cylinder

During one working cycle, which equals two revolutions or $720°$ for a 4-stroke engine, the piston is accelerated by a force due to the gas pressure p in the cylinder as shown in Figure 3a. The second force component acting on the cranktrain are oscillating and rotating mass forces. They are caused by accelerations of piston and conrod and result in inertia forces. The piston is performing an accelerated translational movement in the piston liner, whereas the conrod performs a combined translational and rotational movement. For analytical calculations, the total mass of the conrod is distributed among the piston and the rotating crank pin mass at the crankshaft. The gas force F_{GAS} due to cylinder pressure p and the oscillating mass force F_{OM} sum up to the force acting on the cylinder F_{Z} (see Figure 2).

$$F_{\mathrm{Z}} = F_{\mathrm{GAS}} + F_{\mathrm{OM}} \tag{1}$$

If we define a parameter λ as the ratio of the engine stroke r and the conrod length l

$$\lambda = \frac{r}{l}, \tag{2}$$

we can calculate the tangential force on the cranktrain F_{T} by

$$F_{\mathrm{T}} = F_{\mathrm{Z}} \cdot \left(\sin(\psi) + \frac{\lambda \cdot \sin(\psi) \cdot \cos(\psi)}{\sqrt{1 - \lambda^2 \cdot \sin^2(\psi)}} \right). \tag{3}$$

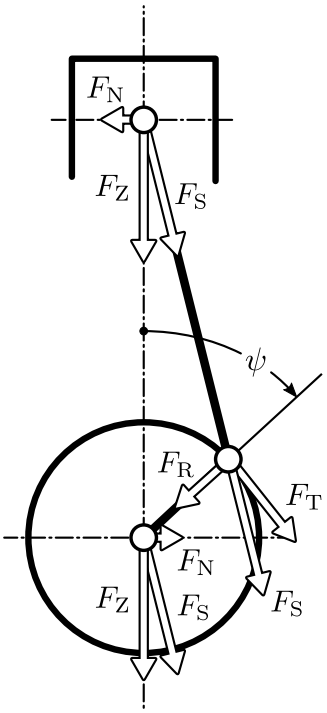

Figure 2: Forces acting on a single cylinder cranktrain [8, p. 42].

For reasons of space we do not go into further details about the analytic formulas of the tribological system and refer to [8, pp. 42] and [9] for a comprehensive overview. The forces acting on the cranktrain of a MAN V48/60CR engine are shown in Figure 2.

Each of the forces can be split into harmonic components utilizing a fast Fourier transform (FFT) as shown in Figure 3.

The tangential crank pin force F_{T} serves as an example force. Through the crankshaft, the forces are transferred to the engine structure, i.e. the crankcase, by the main bearings and form together with the forces in the combustion chamber and the piston normal force F_{N} the excitation forces of the engine structure. A few notes about the excitation:

- Excitation forces are typically calculated by analytical formulas and later one used for various analysis.
- Forces are calculated for a single cylinder and superimposed for the full engine setup, e.g. a 7L or a 12V engine, considering the corresponding phase angles between the cranks and the cylinder firing order.
- FFT results are typically given over engine orders instead of frequencies ([Hz]), since the order does not depend on the actual engine speed. The first order is defined as the engine's rotational speed. For four-stroke engines, the forces are periodic after $720°$, which equals two engine revolutions. Therefore,

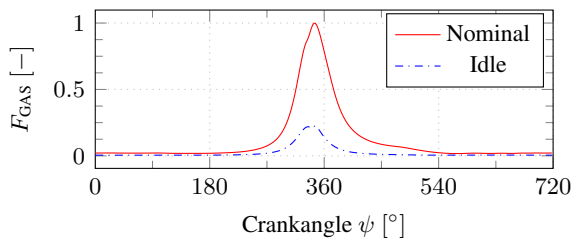

(a) Cylinder pressure force F_{GAS}.

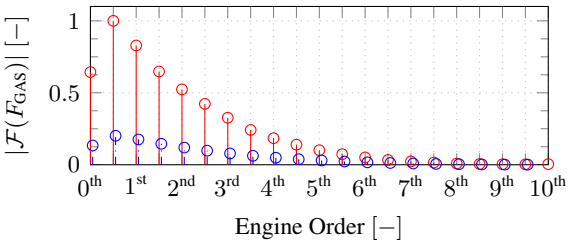

(b) Magnitude of FFT of cylinder pressure force $|\mathcal{F}(F_{GAS})|$.

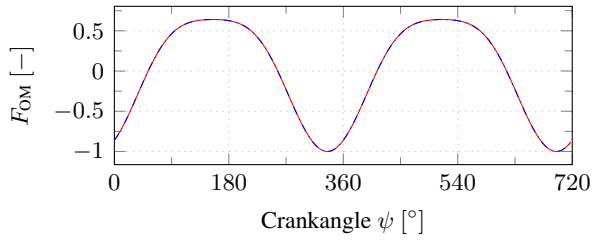

(c) Oscillating mass force F_{OM}.

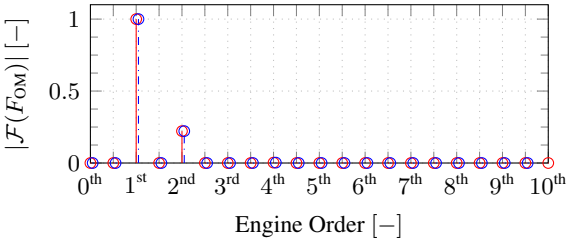

(d) Magnitude of FFT of oscillating mass force $|\mathcal{F}(F_{OM})|$.

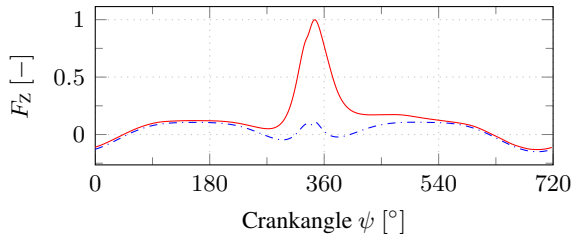

(e) Cylinder force F_Z.

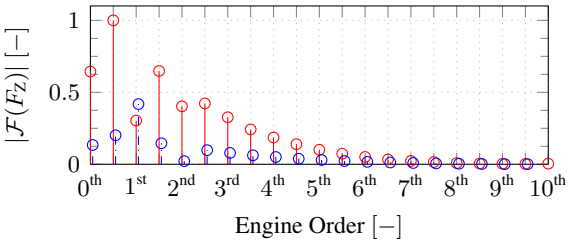

(f) Magnitude of FFT of cylinder force $|\mathcal{F}(F_Z)|$.

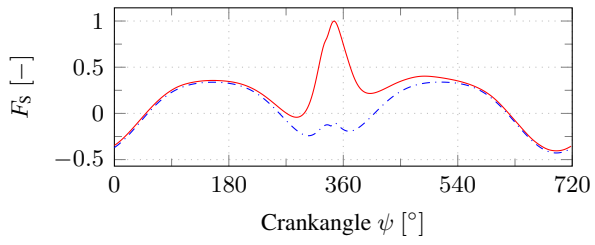

(g) Conrod force F_S.

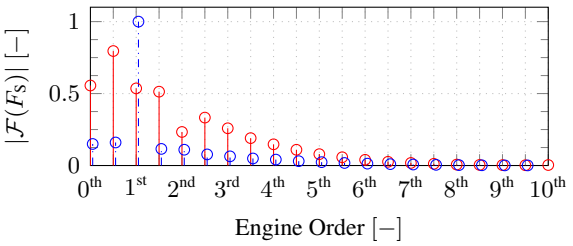

(h) Magnitude of FFT of conrod force $|\mathcal{F}(F_S)|$.

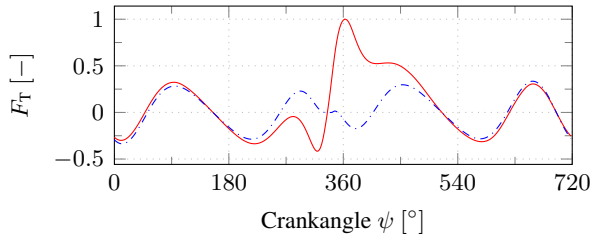

(i) Crank pin tangential force F_T.

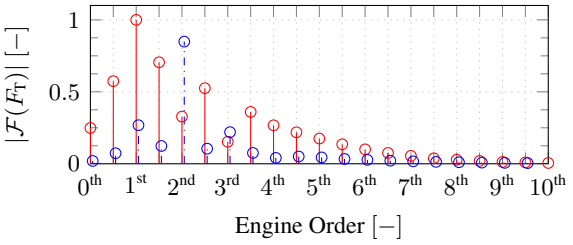

(j) Magnitude of FFT of crank pin tangential force $|\mathcal{F}(F_T)|$.

Figure 3: Forces acting on a single cylinder cranktrain during one working cycle [8]. All values are taken from a MAN V48/60CR engine operating at $514\,\mathrm{rpm}$. Curves are shown for operation at nominal ($85\,\%$) and idle load ($0\,\%$).

0.5^{th} orders appear and constitute the lowest excitation frequency. In contrast, for two-stroke engines only integer orders exist.

- The excitation amplitude is diminishing with high engine orders. It is common to terminate the excitation considered in a vibration analysis after a given number of harmonics. Typically, harmonics up to the 10^{th} or 12^{th} order are considered for engine vibration analysis.

The here presented forces are supposed to give an overview about the most important cranktrain forces and as an illustration of the excitation mechanisms. For a full overview about all forces acting on the cranktrain and the crankcase, we refer again to literature, e.g. [8, 9].

2.1.2 Multi-Cylinder Arrangements

Usually, several cylinders are aligned at a common crankshaft. Depending on the application and the power needs, a varying number of cylinders is used either as in-line (L) engine, meaning there is one crank per cylinder or as vee engine (V), where two conrods share one crank pin. In Figure 4, the schematic crankshaft of a MAN 12V48/60CR engine is shown together with crankstars of several orders that are important in the context of this work.

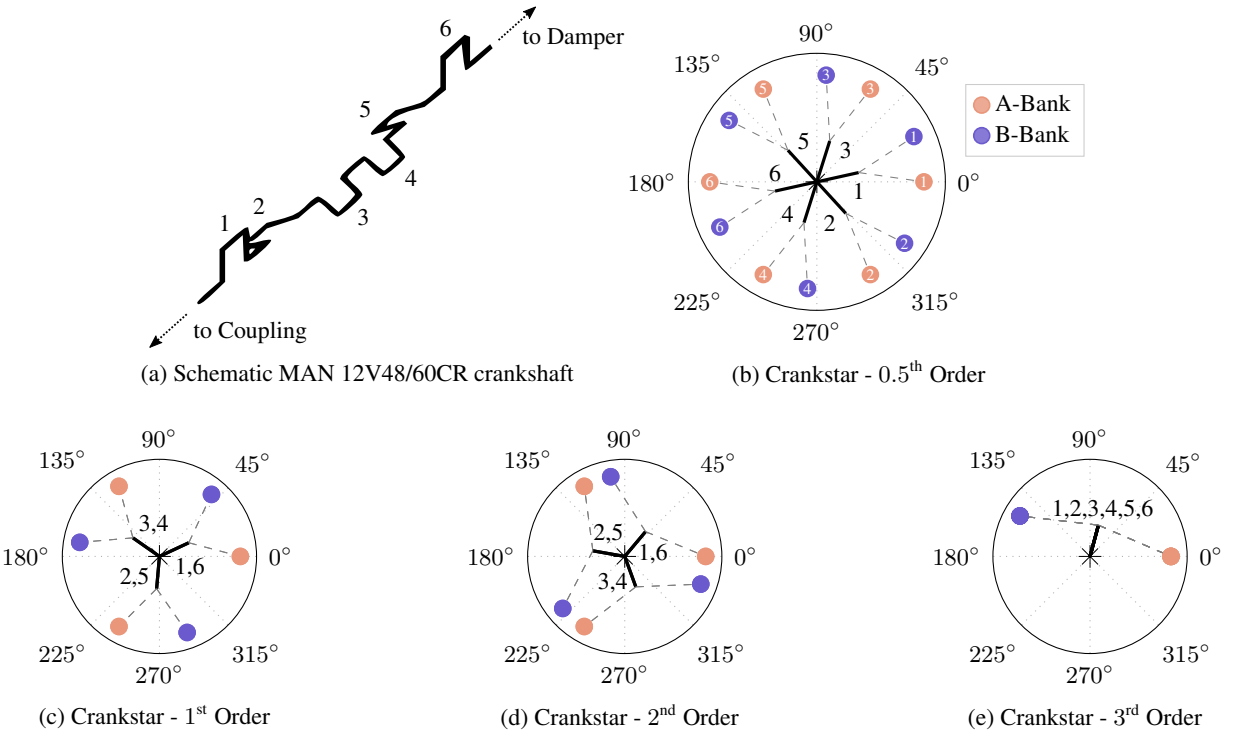

(a) Schematic MAN 12V48/60CR crankshaft

(b) Crankstar - 0.5^{th} Order

(c) Crankstar - 1^{st} Order

(d) Crankstar - 2^{nd} Order

(e) Crankstar - 3^{rd} Order

Figure 4: Schematic MAN 12V48/60CR crankshaft adapted from [8, p. 142] together with a selection of crankstars.

A crankstar is a polar plot of the engine's crank pin orientations along the crankshaft when looking on the crankshaft axis, i.e. the crankshaft axis is positioned perpendicular to the drawing plane. Crankstars can be drawn for a specific harmonic of the engine excitation force (see Figure 3b). The 1^{st} order crankstar equals the geometric arrangement of the crank pins. The crankstars for other harmonics are obtained by multiplying the order of the harmonic with the geometric angle of the crank pin on the crankshaft. A particular feature of the crankstar for the 0.5^{th} order (Figure 4b) for example is that it equals the firing angles of the cylinders and thereby defines the firing order.

From an analytical point of view, V-engines can be treated as two separate in-line engines that operate on the same crankshaft with a phase shift between the cylinder banks which equals the V-angle.

The forces described in Section 2.1.1 are acting at every cylinder and have to be superimposed for the multi-cylinder engine. Superposition is simplified significantly by using frequency domain methods. In frequency domain, superposition is done by summation of the complex amplitudes of the different forces for each harmonic.

After a rough overview of the excitation properties in this section, we will go on with the transmission system in the next section.

2.2 Dynamic properties

The engine behaves as a dynamic system that is excited by forces acting on the cranktrain and the crankcase during the combustion process, as described in Section 2.1. In this section we discuss the dynamic properties of the engine and how they are handled during the engine design process.

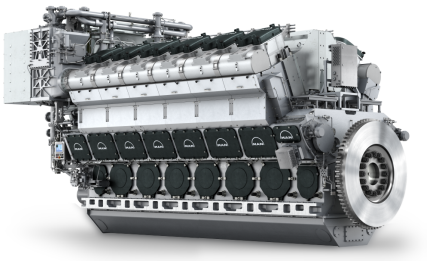

Figure 5: MAN 12V48/60CR

Table 2: MAN 12V48/60CR - Key Figures

Feature	Value	Unit
Bore	480	mm
Stroke	600	mm
Speed	500 / 514	rpm
Power	1080 / 1200	kW/cylinder
Length	10 790	mm
Width	4730	mm
Height	5500	mm
Dry mass	189	t

As example engine we use a MAN 12V48/60CR engine as shown in Figure 5. In Table 2 key figures and properties are listed.

The dynamic properties of the engine can be obtained by Modal Analysis using a finite element method (FEM) software. Those properties consist of natural frequencies $\boldsymbol{f} = \frac{1}{2\pi} \cdot \boldsymbol{\omega}$ (eigenfrequencies) and the corresponding matrix of mode shapes $\boldsymbol{\Phi}$. Starting by the general dynamic equation for a mechanical system [10]

$$\boldsymbol{M}\ddot{\boldsymbol{x}}(t) + \boldsymbol{D}\dot{\boldsymbol{x}}(t) + \boldsymbol{K}\boldsymbol{x}(t) = \boldsymbol{0} \tag{4}$$

with mass matrix $\boldsymbol{M}$, damping matrix $\boldsymbol{D}$, stiffness matrix $\boldsymbol{K}$, displacements $\boldsymbol{x}$ and time t. The equation for the undamped system is given by

$$\boldsymbol{M}\ddot{\boldsymbol{x}}(t) + \boldsymbol{K}\boldsymbol{x}(t) = \boldsymbol{0}. \tag{5}$$

Assuming a linear system, free vibrations will have a harmonic form like

$$\boldsymbol{x}(t) = \boldsymbol{\phi}_r \cos(\omega_r t). \tag{6}$$

Using this ansatz function we get

$$(-\omega_r^2 \boldsymbol{M} + \boldsymbol{K})\boldsymbol{\phi}_r = \boldsymbol{0}. \tag{7}$$

This equation is fulfilled either by the trivial solution $\boldsymbol{\phi}_r = \boldsymbol{0}$ or a non trivial solution, which leads to the undamped eigenvalue problem

$$|\boldsymbol{K} - \omega^2 \boldsymbol{M}| = 0. \tag{8}$$

Nowadays, a variety of numerical tools [10, 11] are available to calculate the solution to this problem in a straightforward way, leading to pairs of angular eigenfrequencies ω_r and eigenmodes $\boldsymbol{\phi}_r$ that fulfill (7).

We obtain the matrix of mode shapes $\boldsymbol{\Phi}$ by arranging the modes $\boldsymbol{\phi}_r$ as column vectors of the matrix

$$\boldsymbol{\Phi} = \begin{bmatrix} | & | & & | \\ \boldsymbol{\phi}_1 & \boldsymbol{\phi}_2 & \cdots & \boldsymbol{\phi}_N \\ | & | & & | \end{bmatrix} \tag{9}$$

for a number of N modes, according to the number of degrees of freedom (DOFs) of the system.

In this paper, we assume that $\boldsymbol{\Phi}$ contains mass-normalized eigenmodes that fulfill the conditions

$$\boldsymbol{\Phi}^T \boldsymbol{M} \boldsymbol{\Phi} = \boldsymbol{I} = \begin{bmatrix} 1 & & 0 \\ & \ddots & \\ 0 & & 1 \end{bmatrix} \tag{10}$$

$$\boldsymbol{\Phi}^T \boldsymbol{K} \boldsymbol{\Phi} = \mathrm{diag}(\boldsymbol{\omega} \odot \boldsymbol{\omega}) = \mathrm{diag}(\boldsymbol{\omega}^2) = \begin{bmatrix} \omega_1^2 & & 0 \\ & \ddots & \\ 0 & & \omega_N^2 \end{bmatrix} \tag{11}$$

where $\boldsymbol{I}$ is the identity matrix and $\odot$ the Hadamard product, i.e. the element-wise product between the elements of the two $\boldsymbol{\omega}$ vectors.

Figure 6 visualizes the six Resilient Mounting Eigenmodes [12, 13] of the MAN 12V48/60CR engine.

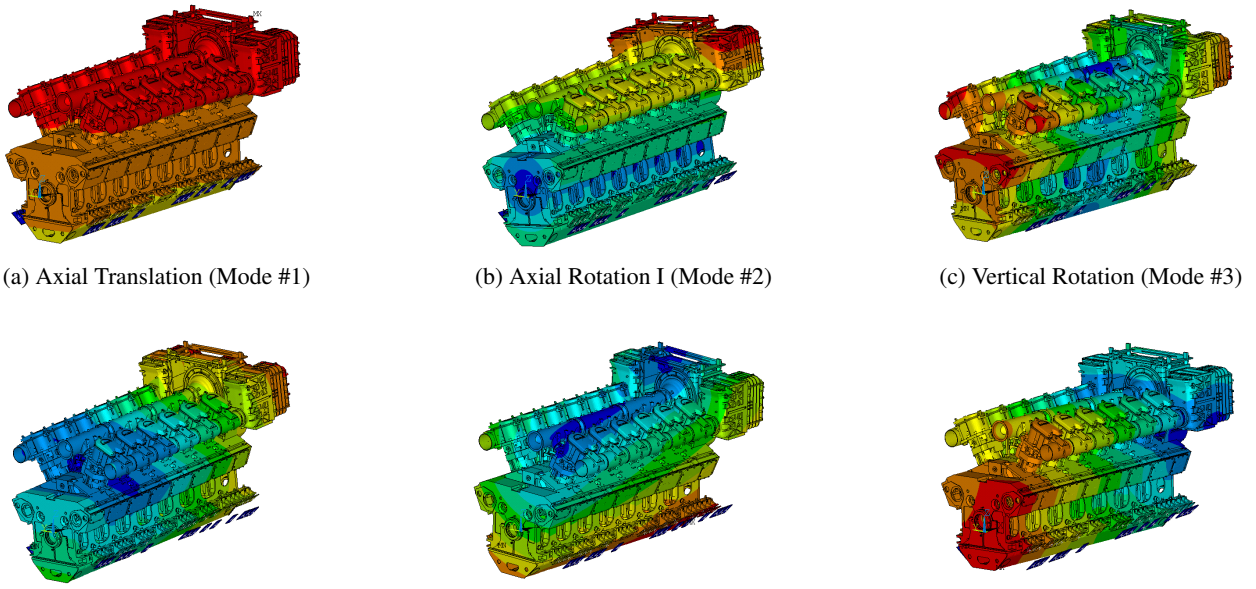

(a) Axial Translation (Mode #1)

(b) Axial Rotation I (Mode #2)

(c) Vertical Rotation (Mode #3)

(d) Cross Directional Rotation (Mode #4)

(e) Axial Rotation II (Mode #5)

(f) Vertical Translation (Mode #6)

Figure 6: Resilient Mounting Eigenmodes of a MAN 12V48/60CR engine. Analysis includes all relevant parts of the engine structure and the resilient mounting joints without further couplings to the surrounding.

Between the Resilient Mounting Eigenmodes and the remaining Elastic Engine Modes there lies a significant gap regarding their eigenfrequencies due to the far lower stiffness of the rubber elements compared to the stiffness of the engine structure. This gap leads to the common assumption of treating Resilient Mounting and Elastic Engine Modes separately in the mount layout or vibration analysis process. In this

context, it is a common approach to simplify the engine model by treating the engine as a rigid body. This assumption dramatically reduces the model's number of DOFs to only 6. The simplification seems to be valid, since due to the large difference in stiffness between the rubber mounts and the engine structure ($\approx$ 3 orders of magnitude), the engine is behaving very similar to a rigid body. This can be seen by calculating the modal assurance criterion (MAC) between the rigid and elastic model as in Figure 7c. Therefore, in the combustion engine context we refer to Resilient Mounting Eigenmodes as quasi-rigid body modes (QRBMs).

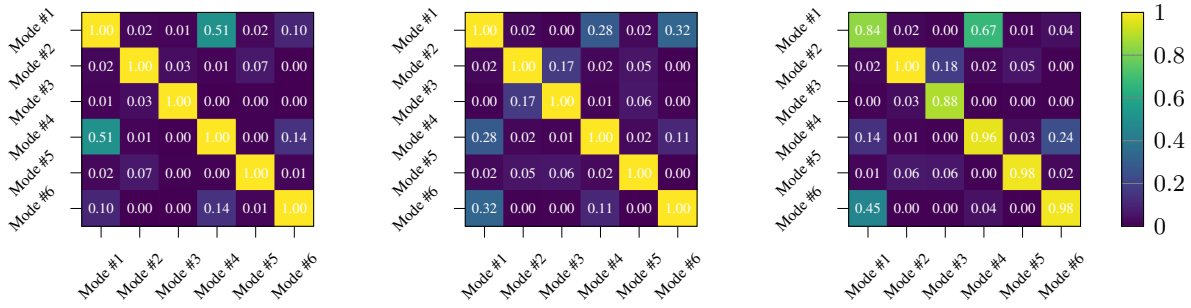

(a) Auto-MAC: Rigid Model (b) Auto-MAC: Elastic Model (c) MAC: Rigid versus Elastic Model

Figure 7: Auto-MAC and MAC matrices for QRBMs for the rigid and elastic engine model.

2.3 Forced Response Analysis

In Section 2.2 we discussed the natural solution of the dynamic system given by (4), which results in the system's eigenfrequencies and eigenmodes, i.e. the system's modal model. In this section, we will explain the solution of the system to a general time-varying force excitation $\mathbf{f}(t)$, as e.g. shown in Figure 3e. This procedure is called Forced Response Analysis (FRA) [14, 15, 16] and calculates a solution to the equation

$$\boldsymbol{M}\ddot{\boldsymbol{x}}(t) + \boldsymbol{D}\dot{\boldsymbol{x}}(t) + \boldsymbol{K}\boldsymbol{x}(t) = \mathbf{f}(t) \tag{12}$$

Further, we now consider the damping matrix $\boldsymbol{D}$ in the solution.

Using the modal transformation [14, pp. 17]

$$\boldsymbol{x}(t) = \boldsymbol{\Phi}\boldsymbol{q}(t) \tag{13}$$

we can calculate the response of the system $\boldsymbol{x}(t)$ as superposition of the systems eigenmodes $\boldsymbol{\Phi}$. $\boldsymbol{q}(t)$ is called the modal response of the system and can be interpreted as weighting factor for the modes $\boldsymbol{\Phi}$ [14].

If we insert (13) into (12) and left multiply by $\boldsymbol{\Phi}^T$ we get

$$\boldsymbol{\Phi}^T\boldsymbol{M}\boldsymbol{\Phi}\ddot{\boldsymbol{q}}(t) + \boldsymbol{\Phi}^T\boldsymbol{D}\boldsymbol{\Phi}\dot{\boldsymbol{q}}(t) + \boldsymbol{\Phi}^T\boldsymbol{K}\boldsymbol{\Phi}\boldsymbol{q}(t) = \boldsymbol{\Phi}^T\mathbf{f}(t) \tag{14}$$

$$= \ddot{\boldsymbol{q}}(t) + \boldsymbol{L}\dot{\boldsymbol{q}}(t) + \mathrm{diag}(\boldsymbol{\omega}^2)\boldsymbol{q}(t) = \boldsymbol{\Phi}^T\mathbf{f}(t) \tag{15}$$

where $\boldsymbol{L}$ is the generalized damping matrix. If we choose a viscous damping model like the Rayleigh-Damping model [17, p. 17]

$$\boldsymbol{D} = \alpha\boldsymbol{M} + \beta\boldsymbol{K} \tag{16}$$

that defines the damping matrix $\boldsymbol{D}$ as a linear combination of mass matrix $\boldsymbol{M}$ and stiffness matrix $\boldsymbol{K}$ with multipliers α and β and substitute into (14), we get for the damping term

$$\boldsymbol{L}\dot{\boldsymbol{q}}(t) = \boldsymbol{\Phi}^T \boldsymbol{D} \boldsymbol{\Phi} \dot{\boldsymbol{q}}(t) = \boldsymbol{\Phi}^T [\alpha \boldsymbol{M} + \beta \boldsymbol{K}] \boldsymbol{\Phi} \dot{\boldsymbol{q}}(t) = [\alpha \boldsymbol{I} + \beta \operatorname{diag}(\boldsymbol{\omega}^2)] \dot{\boldsymbol{q}}(t). \tag{17}$$

The term after the last equality sign is obtained by utilizing the orthogonality conditions in (10) and (11).

By using a Rayleigh-Damping approach, the equations of the dynamic system are decoupled [14]. This circumstance enables the superposition of the generalized DOFs $q_r(t)$. Due to the decoupling and the analogy to a single degree of freedom (SDOF) system, we can replace the modal damping equation by

$$\alpha + \beta \omega_r^2 = 2 \xi \omega_r \tag{18}$$

where ξ is the damping ratio according to Lehr [14]. If we substitute (17) and (18) in (14), we get

$$\ddot{\boldsymbol{q}}(t) + 2 \operatorname{diag}(\boldsymbol{\xi} \odot \boldsymbol{\omega}) \dot{\boldsymbol{q}}(t) + \operatorname{diag}(\boldsymbol{\omega}^2) \boldsymbol{q}(t) = \boldsymbol{\Phi}^T \mathbf{f}(t) \tag{19}$$

where $\boldsymbol{\xi}$ is the vector of damping ratios ξ_r corresponding to eigenmode ϕ_r and angular eigenfrequency ω_r.

We can choose again harmonic ansatz functions for the modal response and the excitation forces

$$\boldsymbol{q}(t) = \hat{\boldsymbol{q}} e^{i\Omega t} \tag{20}$$

$$\mathbf{f}(t) = \hat{\mathbf{f}} e^{i\Omega t} \tag{21}$$

where $\hat{\boldsymbol{q}}$ and $\hat{\mathbf{f}}$ are complex valued amplitudes. By substituting into (19), we get

$$-\Omega^2 \hat{\boldsymbol{q}} + i\Omega [2 \operatorname{diag}(\boldsymbol{\xi} \odot \boldsymbol{\omega})] \hat{\boldsymbol{q}} + \operatorname{diag}(\boldsymbol{\omega}^2) \hat{\boldsymbol{q}} = \boldsymbol{\Phi}^T \hat{\mathbf{f}} \tag{22}$$

Through factorizing for $\hat{\boldsymbol{q}}$ and solving for the unknown, (22) becomes

$$\hat{\boldsymbol{q}} = \frac{\boldsymbol{\Phi}^T \hat{\mathbf{f}}}{\operatorname{diag}(\boldsymbol{\omega}^2) - \Omega^2 \boldsymbol{I} + i\Omega [2 \operatorname{diag}(\boldsymbol{\xi} \odot \boldsymbol{\omega})]}. \tag{23}$$

Using a re-transformation into time-domain with

$$\boldsymbol{x}(t) = \hat{\boldsymbol{x}} e^{i\Omega t} = \boldsymbol{\Phi} \hat{\boldsymbol{q}} e^{i\Omega t} \Rightarrow \hat{\boldsymbol{q}} = \boldsymbol{\Phi}^{-1} \hat{\boldsymbol{x}} \tag{24}$$

we obtain the solution of the dynamic system

$$\hat{\boldsymbol{x}} = \boldsymbol{\Phi} \frac{\boldsymbol{\Phi}^T \hat{\mathbf{f}}}{\operatorname{diag}(\boldsymbol{\omega}^2) - \Omega^2 \boldsymbol{I} + i\Omega [2 \operatorname{diag}(\boldsymbol{\xi} \odot \boldsymbol{\omega})]}. \tag{25}$$

Equation (25) together with a sum notation and time-differentiation leads to an equation for the SBN velocity $\hat{v}$ at DOF j in response to the complex excitation vector $\hat{\mathbf{f}}$.

$$\hat{v}_j e^{i\Omega t} = \frac{\mathrm{d}(\hat{x}_j e^{i\Omega t})}{\mathrm{d}\, t} = i\Omega \sum_{r=1}^{N} \frac{(\boldsymbol{\phi}_r)_j (\boldsymbol{\phi}_r^T \hat{\mathbf{f}})}{\omega_r^2 - \Omega^2 + i 2 \xi_r \omega_r \Omega} e^{i\Omega t} \tag{26}$$

Equation (26) is called Harmonic Response Formula [14, p. 17] in the context of this work. Some remarks regarding this equations:

- $\hat{v}_j$ is the velocity vibration amplitude at DOF j.

- Ω ist the angular frequency for which the vibration velocity is calculated.
- $\boldsymbol{\omega}$ is the vector of angular natural frequencies, i.e. angular eigenfrequencies, of the system.
- $(\boldsymbol{\phi}_r)_j$ is the value of mode shape $(\boldsymbol{\phi}_r)$ at DOF j.
- i is the complex unit.
- ξ_r is the damping ratio according to Lehr corresponding to mode $(\boldsymbol{\phi}_r)$ and angular eigenfrequency ω_r. Using the Harmonic Response Formula, it is possible to define individual damping ratios for each mode. However, it is common to use a single value throughout the analysis.
- $\hat{\mathbf{f}}$ contains the complex valued excitation forces at each DOF corresponding to the angular evaluation frequency Ω.

For the Response Analysis of an engine, (26) is typically calculated for different engine speeds. Further, the Harmonic Response Formula calculates the response only for a single angular frequency Ω with corresponding force vector $\hat{\mathbf{f}}_\Omega$. However, for an IC engine there are a number of frequencies acting at the same time, as we have shown in Figure 3. To cover the full engine excitation, we have to calculate the Harmonic Response for each engine order k ($0.5^{\text{th}}, 1.0^{\text{st}}, 1.5^{\text{th}}, \ldots$) at each engine speed u.

This leads to an extended Harmonic Response Formula

$$\hat{v}_{j,k}(\Omega) = i\Omega_k \sum_{r=1}^{N} \frac{(\boldsymbol{\phi}_r)_j (\boldsymbol{\phi}_r^T \hat{\mathbf{f}}_k)}{\omega_r^2 - \Omega_k^2 + i2\xi_r\omega_r\Omega_k} \tag{27}$$

where k is the excitation order and Ω_k the angular frequency adjusted for the current order k

$$\Omega_k = k \cdot \Omega; \qquad k \in K; \qquad K = \{0.5, 1.0, 1.5, \ldots\} \tag{28}$$

With (27), we can calculate the engine response at each DOF j for each mode i at each engine speed Ω for each excitation order k. This formula gives a good impression about the properties and complexity of an IC engine in regards of dynamic systems. To ease the assessment of vibration velocities, it is common to calculate the root mean square (RMS) of $\hat{v}_j$ over all engine orders.

$$\hat{v}_{j,\text{RMS}}(\Omega) = \sqrt{\frac{1}{2}\sum_{k\in K}\left(\left| i\Omega_k \sum_{r=1}^{N} \frac{(\boldsymbol{\phi}_r)_j (\boldsymbol{\phi}_r^T \hat{\mathbf{f}}_k)}{\omega_r^2 - \Omega_k^2 + i2\xi_r\omega_r\Omega_k} \right|^2\right)} \tag{29}$$

To further analyze (26), it can be factorized into sub-equations for which we can find a particular physical meaning. Those are shown in (30) and (31).

$$C_{r,k} = (\boldsymbol{\phi}_r^T \hat{\mathbf{f}}_k) = \boldsymbol{\phi}_r \cdot \hat{\mathbf{f}}_k = \sum_{l=1}^{N} \phi_{r,l} \cdot \hat{\mathrm{f}}_{k,l} \tag{30}$$

$$R_{r,k}(\Omega) = i\Omega_k \frac{1}{\omega_r^2 - \Omega_k^2 + i2\xi_r\omega_r\Omega_k} \tag{31}$$

$C_{r,k}$ is called Excitation Criterion. It depends only on the current mode $\boldsymbol{\phi}_r$ and the force $\hat{\mathbf{f}}_k$ for order k. We can interpret the criterion as condition for the excitation of mode $\boldsymbol{\phi}_r$ under the given force vector $\hat{\mathbf{f}}_k$. From algebra we know, that the criterion is 0 if either the force vector equals the zero vector $\hat{\mathbf{f}}_k = \mathbf{0}$ or the mode and the force are orthogonal. If the criterion becomes $C_{r,k} = 0$, the response for mode i and order k will be zero as well. Apart from the Criterion Value $C_{r,k}$, we can define $R_{r,k}(\Omega)$ as the Resonance Value. $R_{r,k}(\Omega)$ depends on the engine speed Ω, excitation order k, eigenfrequency ω_r and damping ratio ξ_r. However, it is independent of force vector $\hat{\mathbf{f}}_k$. It describes the amplification of the response at the angular frequency Ω_k depending on the distance to the resonance frequency of mode i, i.e. the angular natural frequency ω_r.

Excitation Criterion $C_{r,k}$ and Resonance Value $R_{r,k}(\Omega)$ can be evaluated separately and then assembled together into the overall response formula (see (26)). If we ignore the factor $(\phi_r)_j$, which is necessary to obtain the response at DOF j, we can define the generalized response for mode i as

$$\tilde{v}_{r,k}(\Omega) = C_{r,k} R_{r,k}(\Omega) \tag{32}$$

which enables us to write the response (26) as

$$\hat{v}_{j,k}(\Omega) = \sum_{r=1}^{N} (\phi_r)_j (\tilde{v}_{r,k}(\Omega)) = \sum_{r=1}^{N} (\phi_r)_j C_{r,k} R_{r,k}(\Omega) \tag{33}$$

In Section 3, we use the QRBMs from a 12V48/60CR engine shown in Figure 6 and the FRA, which we described here, to analyze the excitation properties of the system. A special focus is set on the common model simplification of assuming the engine structure to be a rigid body.

3 Results

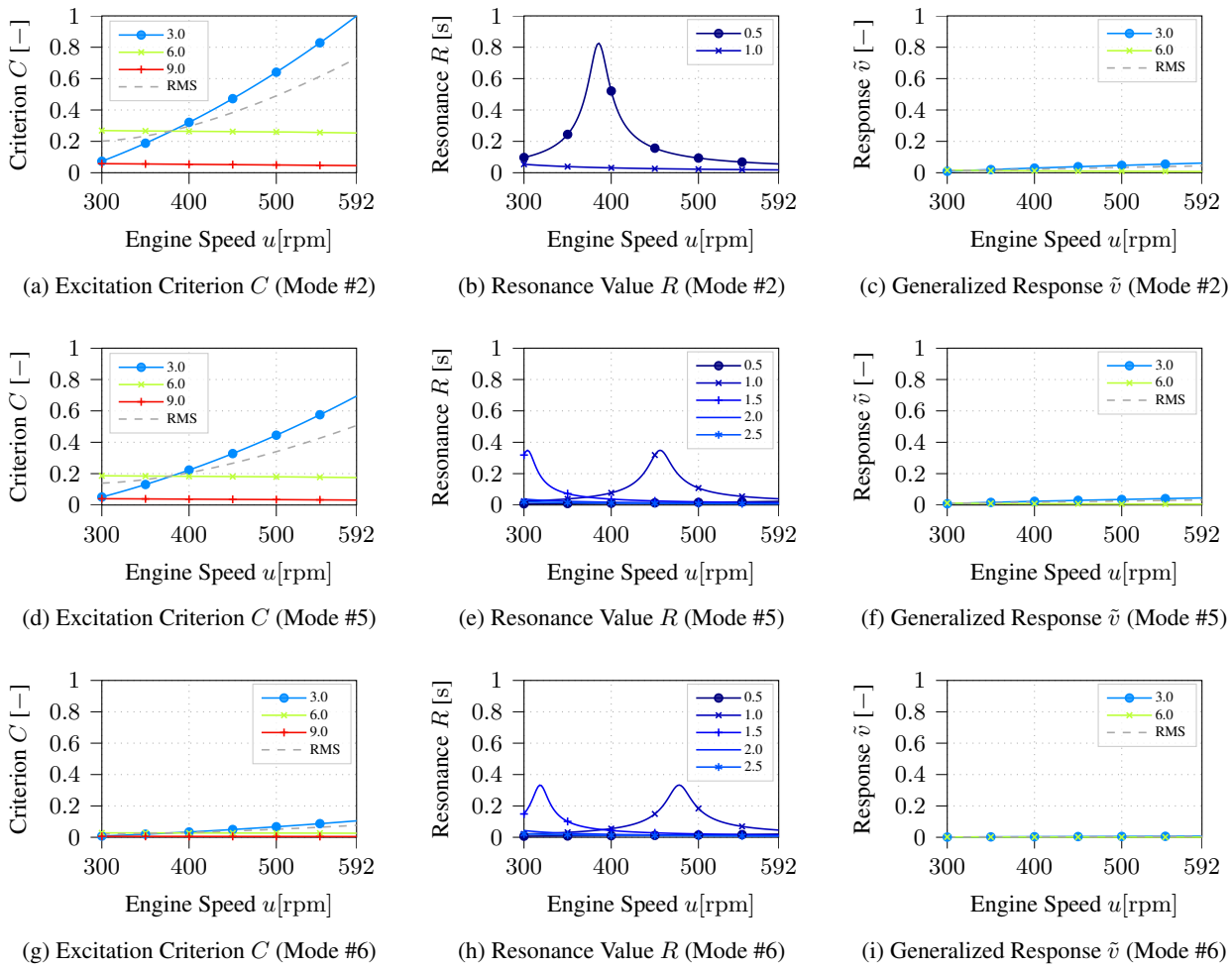

(a) Excitation Criterion C (Mode #2) (b) Resonance Value R (Mode #2) (c) Generalized Response $\tilde{v}$ (Mode #2)

(d) Excitation Criterion C (Mode #5) (e) Resonance Value R (Mode #5) (f) Generalized Response $\tilde{v}$ (Mode #5)

(g) Excitation Criterion C (Mode #6) (h) Resonance Value R (Mode #6) (i) Generalized Response $\tilde{v}$ (Mode #6)

Figure 8: Response Analysis for QRBMs #2, #5 and #6 of the rigid MAN 12V48/60CR engine model shown for the most dominant engine orders.

To analyze the vibration behavior of the engine's QRBMs, we use a Forced Response Analysis (FRA) as described in Section 2.3. In the last section, we have shown that the Harmonic Response Formula in (26) can

be divided into sub-equations (30) and (31), which can be treated independently from each other. To analyze the response, we can consider them separately, in order to get deeper insights into the excitation mechanisms of the underlying system. As shown in (32), we can afterwards calculate a generalized response $\tilde{v}_{r,k}(\Omega)$ for each mode ϕ_r, for analyzing the contribution of each mode to the overall response $\hat{v}_{j,k}(\Omega)$.

We start by calculating the criterion $C_{r,k}$, the resonance value $R_{r,k}(\Omega)$ and the generalized response $\tilde{v}_{r,k}$ for the QRBMs of the rigid model.

The calculated values are illustrated in Figure 8. We can note the following points:

- Only the results for QRBMs #2, #5 and #6 are plotted, because the excitation for the remaining modes is negligible small, so we can neglect their contribution to the overall response.
- Further, we plot only engine orders k that lie over a certain threshold value. E.g. for the excitation criterion C we plot only orders whose maximum value lies over a threshold (here $5\,\%$) compared to the maximum value of all orders. The same applies for the resonance values R and the generalized response $\tilde{v}$. This helps to keep the plots reasonable, otherwise there would be ≈ 20 curves in each plot of which only a few are relevant.
- Criterion C and generalized response $\tilde{v}$ are normalized to the corresponding maximum value among all modes of the rigid and the elastic model. This simplifies the comparison between the two modeling approaches.

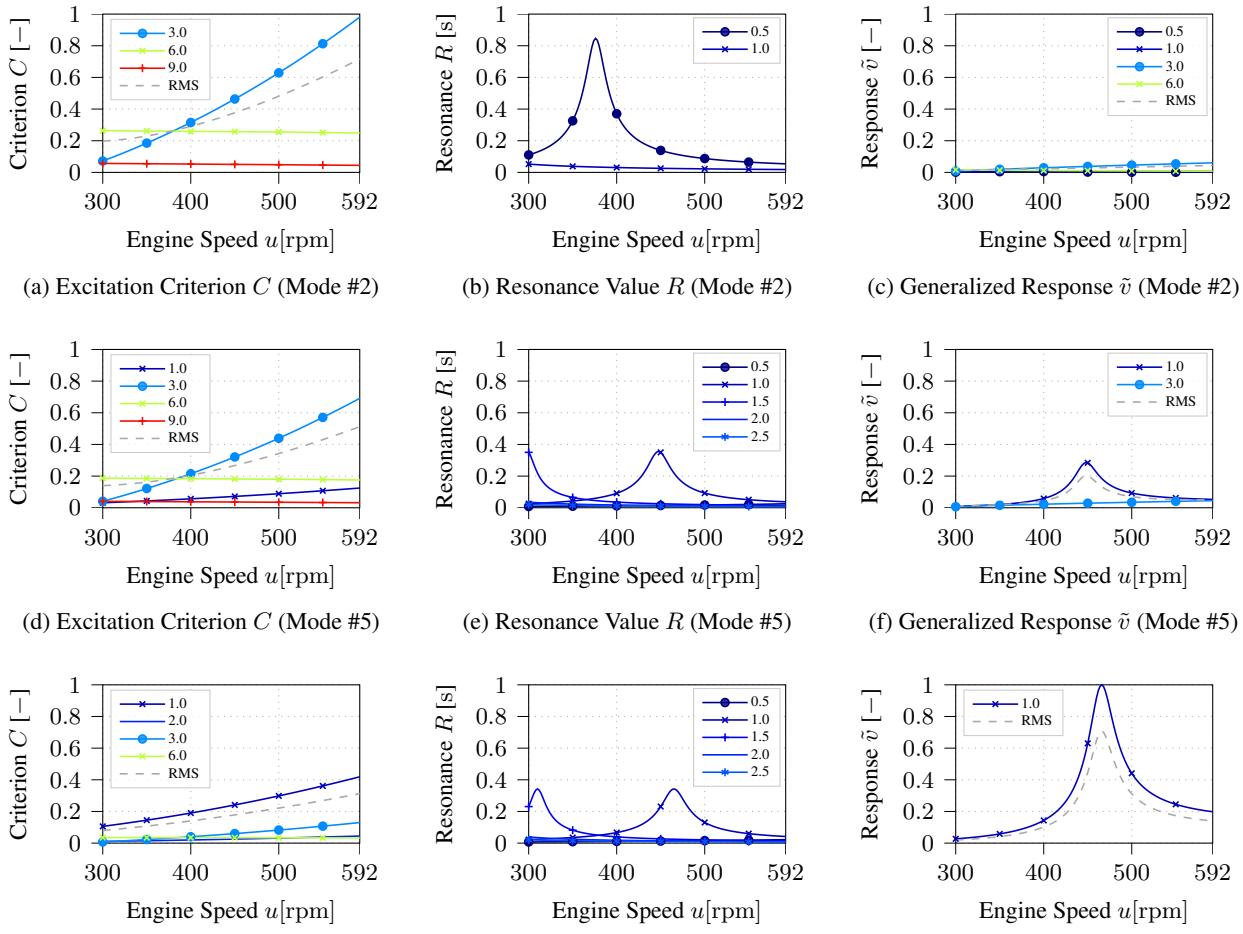

(a) Excitation Criterion C (Mode #2) (b) Resonance Value R (Mode #2) (c) Generalized Response $\tilde{v}$ (Mode #2)

(d) Excitation Criterion C (Mode #5) (e) Resonance Value R (Mode #5) (f) Generalized Response $\tilde{v}$ (Mode #5)

(g) Excitation Criterion C (Mode #6) (h) Resonance Value R (Mode #6) (i) Generalized Response $\tilde{v}$ (Mode #6)

Figure 9: Response Analysis for QRBMs #2, #5 and #6 of the elastic MAN 12V48/60CR engine model shown for the most dominant engine orders.

From the criterion plots C, we can see that only the 3$^{\text{rd}}$ order and integer multiples of it deliver excitation for

the corresponding QRBMs. This is in accordance with the common theory [8, 9] for multi-cylinder engines, as described in Section 2.1.2. For a MAN 12V48/60CR engine, the crank pins are arranged in a way, that along the crankshaft axis harmonic force components of the individual cylinders eliminate each other for all engine orders except the 3rd and its integer multiples. This can be directly seen, when visualizing the crankstars for each engine order. The crankstars for the 1st and 2nd are shown in Figures 4c and 4d. We can see that the crank pins are arranged symmetrically, leading to an elimination of forces for the corresponding order. The same applies for all other crankstars, except for the 3rd engine order. Here, all crank pins point into the same direction, meaning that the forces are not compensated within the engine, but cause forces and moments to the surrounding structure and can possibly excite QRBMs. Since the resonance frequency for the 3rd order lies outside the relevant speed range for the QRBMs, there is no significant excitation compared to the remaining elastic modes of the engine. The engine in this example (MAN 12V48/60CR) is said to have no free forces and moments, meaning in summation there is no excitation in the 1st and 2nd order.

In summary, following the analytical engine theory, which assumes rigid cranktrain models, and the results from the analysis shown in Figure 8, one would not expect a significant excitation of QRBMs in the relevant speed range for a MAN 12V48/60CR engine.

If we carry out the RA for the elastic model, we can see in Figures 9d and 9g that an excitation in the 1st order appears, that was not observed for the rigid model. Since the eigenfrequencies between the two modelling approaches are very similar, the resonance values in the middle column of Figure 9 are almost identical to the rigid model in Figure 8. Finally, for the generalized response, we can now observe significant excitation of modes #5 and #6. This is surprising, since the excitation of QRBMs is unexpected following the established engine theory. As we observe excitation in the 1st order for the criterion C in Figures 9d and 9g and a resonance of the corresponding modes in the relevant speed range in Figures 9e and 9h, the generalized response $\tilde{v}$ for the modes becomes significant. Due to the normalization of the response levels among all QRBMs for both the rigid and the elastic model, we can see that modes #5 and #6 of the elastic model have the highest response. If we compare the response levels to higher modes of the elastic model, which are - due to reasons of space - not shown here, the response is still comparatively high. We can say modes #5 and #6 are dominant modes in the overall engine response.

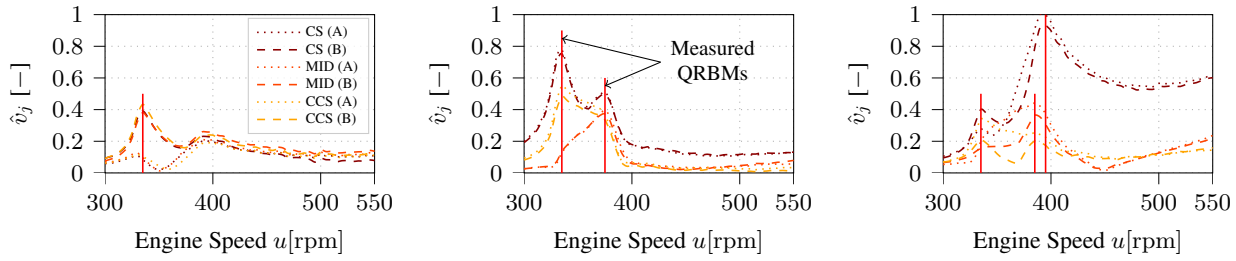

(a) Direction: Axial (b) Direction: Horizontal (c) Direction: Vertical

Figure 10: Order Tracking measurements for 1st order engine velocity amplitudes $\hat{v}_j$ of a MAN 12V48/60CR engine at test bed at different measurement points (MPs) at the engine-sided connection to the resilient mounting. Values are shown for the A-Bank (A) and B-Bank (B) at engine coupling side (CS), midst (MID) and counter-coupling side (CCS). All values are normalized to the common maximum velocity amplitude.

Due to the arrangement of the crank pins for a MAN 12V48/60CR (see Figure 4) and the assumption of a rigid model, the vectors $\boldsymbol{\phi}_r$ and $\hat{\mathbf{f}}_k$ in the excitation criterion in (30) become orthogonal and therefore deliver no excitation (see Figure 8, left column) regarding QRBMs, i.e. the components $\phi_{r,l} \cdot \hat{\mathrm{f}}_{k,l}$ eliminate each other during summation. If we add elasticity to the engine structure, we can understand that the orthogonality between the mode and force vector is not strictly fulfilled anymore. However, it is surprising that this small disturbance leads to significant excitation and response values, which become dominating in the overall response. When measuring the vibration velocity amplitudes at test bed this excitation in the 1st engine order is also present as shown in Figure 10.

4 Conclusion

After an introduction of fundamental engine theory including engine excitation due to gas and mass forces, analytical analysis and multi-cylinder arrangements, we discussed the dynamic properties of an IC engine's structure. In a Modal Analysis of a resiliently mounted engine, different groups of modes with specific properties can be identified. Apart from the Elastic Engine Modes, modes originating from the resilient mounting system are found, which play a key role in engine integration. Due to their low eigenfrequencies, that lie in or are close to the operational speed range, they demand careful treatment during the design process. Further, in case of vibration issues, the resilient mounting system can be rather easily modified in comparison to changes in the engine structure. Since the resilient mounting is the main path for SBN transmission from the source (engine) to the receiver (ship/water), the analysis of the corresponding properties is of special interest.

In Sections 2.2 and 2.3, we presented the dynamic properties of a MAN 12V48/60CR engine and the relevant Harmonic Response theory for the further analysis. We introduced the Harmonic Response Formula and showed how it can be separated into individual sub-parts, namely an excitation criterion C, which depends on the mode shape and the exciting force vector, and a resonance value R, that depends on the eigenfrequency of the considered mode. Together with the mode value at a particular DOF $(\boldsymbol{\phi}_r)_j$, the response $\hat{v}_j$ can be calculated. If the particular DOF is ignored and only excitation criterion and resonance value are considered, we can calculate a generalized response $\tilde{v}$ of a given mode.

When looking at the first six eigenmodes of the engine system, due to the difference in stiffness of several orders of magnitude between the resilient mounts and the engine structure, the engine behaves almost like a rigid body. Therefore, we refer to modes due to the resilient mounting as quasi-rigid body modes (QRBMs). Because of this quasi-rigid behavior, it is a common approach in literature to treat the engine as a rigid object, which dramatically reduces the number of DOFs in the model. Many analytical approaches and considerations about engine vibrations and tribology rely on the assumption of a rigid engine structure [8, 9].

In Section 3, we carried out a Response Analysis for a rigid and an elastic engine model. The analysis lead to quite unexpected results. Due to the arrangement of crank pins on the crankshaft there is usually no significant excitation of QRBMs expected. This was proven in the analysis of the rigid model, for which we see a small excitation in the 3^{rd}, 6^{th} and 9^{th} order. The elastic engine model contains a finite element (FE) model of the engine structure. Due to the higher stiffness of the engine compared to the mounts, the mode shapes are only slightly different compared to the rigid model. However, the Response Analysis revealed a high excitation of QRBMs that dominate the engine response in parts of the engine's operational speed range.

To summarize, rigid engine models have to be treated with caution during engine design process. They play a key role in the dimensioning of resilient mounting systems. When considering multi-cylinder engines, depending on the engine type and the number of cylinders, one would not expect a response of QRBMs for a MAN 12V48/60CR engine. However, QRBMs can be observed with a significant contribution to the overall response, when using an elastic engine model. Therefore, for the calculation of operational vibration behavior, elasticity should be carefully considered to understand its influence compared to simplified approaches. In measurements, QRBMs are commonly observed (see Figure 10) and – if they appear in the 1^{st} order – often said to be excited by unbalances in the cranktrain. However, this work proofs that the excitation is intrinsic to the system due to the small disturbance of Resilient Mounting Eigenmodes by engine elasticity.

Acknowledgements

This work is partially funded by the German Federal Ministry for Economic Affairs and Energy within the consortium project 'TSCHALL' (funding code: 03SX468E) in the sub-project 'Structure-Borne Noise on Board'. The project aims on the investigation of low-frequency sound radiation from ships into water excited by main engines. The author is responsible for the content of this work.

References

[1] L. Moro, "Structure borne noise due to marine diesel engines: experimental study and numerical simulation for the prediction of the dynamic behaviour of resilient mounts," Ph.D. dissertation, Università degli studi di Trieste, 2015.

[2] J. A. Hildebrand, "Anthropogenic and natural sources of ambient noise in the ocean," *Marine Ecology Progress Series*, vol. 395, pp. 5–20, 2009.

[3] W. J. Richardson, C. R. Greene Jr, C. I. Malme, and D. H. Thomson, *Marine mammals and noise*. Academic press, 2013.

[4] G. M. Wenz, "Acoustic ambient noise in the ocean: Spectra and sources," *The Journal of the Acoustical Society of America*, vol. 34, no. 12, pp. 1936–1956, 1962.

[5] N. R. Council *et al.*, "Ocean noise and marine mammals," 2003.

[6] IMO, "Guidelines for the reduction of underwater noise from commercial shipping to address adverse impacts on marine life," 2014.

[7] Port of vancouver, "Enhancing cetacean habitat and ovservation (echo) program," https://www.portvancouver.com/environment/water-land-wildlife/echo-program/, accessed: 2020-08-25. [Online]. Available: https://www.portvancouver.com/environment/water-land-wildlife/echo-program/

[8] H. Maass and H. Klier, *Kräfte, Momente und deren Ausgleich in der Verbrennungskraftmaschine*. Springer-Verlag, 1981, vol. 2.

[9] V. Gheorghiu, *Kolbenmaschinen (KoM) und Kolbenverbrennungsmotoren (KVM)*. Hochschule für Angewandte Wissenschaften Hamburg, 2009.

[10] Ansys Inc., *Theory Reference for the Mechanical APDL and Mechanical Applications*, Apr. 2009, release 12.0.

[11] C. R. Harris, K. J. Millman, S. J. van der Walt, R. Gommers, P. Virtanen, D. Cournapeau, E. Wieser, J. Taylor, S. Berg, N. J. Smith, R. Kern, M. Picus, S. Hoyer, M. H. van Kerkwijk, M. Brett, A. Haldane, J. F. del Río, M. Wiebe, P. Peterson, P. Gérard-Marchant, K. Sheppard, T. Reddy, W. Weckesser, H. Abbasi, C. Gohlke, and T. E. Oliphant, "Array programming with NumPy," *Nature*, vol. 585, no. 7825, pp. 357–362, Sep. 2020. [Online]. Available: https://doi.org/10.1038/s41586-020-2649-2

[12] T. Parikyan, N. Naranca, and J. Neher, "Powertrain resilient mounting design analysis," in *Internal Combustion Engine Division Fall Technical Conference*, vol. 51999. American Society of Mechanical Engineers, 2018, p. V002T07A002.

[13] J. Neher, A. Rieß, and M. Basic, "Large engine vibration analysis using a modular modelling approach," AVL - German Simulation Conference 2018, Tech. Rep., 2018.

[14] B. Graf, *Validierung von Methoden zur Berechnung und Reduzierung der Schallabstrahlung von Getriebegehäusen*. Universitätsverlag Ilmenau, 2007.

[15] J. Neher, "Laborunterlagen: Responseanalyse," *Ulm University of Applied Sciences*, Apr. 2018.

[16] J. Neher, *Lecture Script: Schwingungen und Akustik*, Ulm University of Applied Sciences, 2020.

[17] A. Rieß, *Model Order Reduction Based Simulation and Optimization of Large Bore Internal Combustion Engines*. Shaker, 2015.